Cosmogenic neutrinos from cosmic ray interactions with extragalactic infrared photons

Todor Stanev* and Daniel De Marco†
Bartol Research Institute, University of Delaware, Newark, Delaware 19716, USA

M. A. Malkan‡
Department of Physics and Astronomy, University of California, Los Angeles, California 90095, USA

F. W. Stecker§
NASA Goddard Space Flight Center, Greenbelt, Maryland 20771, USA
(Received 22 December 2005; published 16 February 2006)

We discuss the production of cosmogenic neutrinos on extragalactic infrared photons in a model of its cosmological evolution. The relative importance of these infrared photons as a target for proton interactions is significant, especially in the case of steep injection spectra of the ultrahigh energy cosmic rays. For an $E^{-2.5}$ cosmic ray injection spectrum, for example, the event rate of neutrinos of energy above 1 PeV is more than doubled.

DOI: 10.1103/PhysRevD.73.043003 PACS numbers: 98.70.Sa, 13.85.Tp, 98.70.Lt, 98.80.Es

I. INTRODUCTION

The assumption that the ultra high energy cosmic rays (UHECR) are nuclei (presumed here to be protons) accelerated in powerful extragalactic sources provides a natural connection between these particles and ultra high energy neutrinos. This was first realized by Berezinsky and Zatsepin [1] soon after the introduction of the Greisen-Zatsepin-Kuzmin (GZK) effect [2]. The GZK effect is the modification of the UHE proton spectrum from energy losses by photoproduction interactions with the 2.7K microwave background radiation (MBR). In the case of isotropic and homogeneous distribution of UHE cosmic ray sources, the GZK effect leads to a cutoff of the cosmic ray spectrum below 10^{20} eV. The charged mesons generated in these interactions initiate a decay chain that results in neutrinos. Since the mesons and muons do not lose energy before decay, the high energy end of the spectrum of these neutrinos follows the injection spectrum of UHECR, while below the interaction threshold it is flat [3,4]. The neutrinos which are produced by photomeson producing interactions of UHECR nuclei are sometimes referred to as *cosmogenic neutrinos*.

Several calculations of the fluxes of UHE photomeson neutrinos were published in the 1970s [3–7], Hill and Schramm [8,9] used the nondetection of such neutrinos to place an upper limit on the cosmological evolution of the sources of UHECR. The problem has been revisited several more times [10–12].

In 2004 Stanev [13] considered interactions of UHECR with photons of the extragalactic infrared and optical background (IRB), pointing out that this process generates nonnegligible cosmogenic neutrino fluxes. This suggestion was quickly followed by a confirmation in Ref. [14] which emphasized the importance of the IRB as interaction target. This idea was further developed in Ref. [15].

Reference [13] gave an estimate of the cosmogenic neutrino flux generated in interactions on the IRB but did not account correctly for the cosmological evolution of the infrared background. In this paper we perform a calculation using a realistic empirically based model of the cosmological evolution of the spectral energy distribution of the extragalactic IR-UV background given in Ref. [16] which will be referred to as SMS05. The aim is to estimate correctly the role of these extragalactic photons, particularly the infrared photons which are by far the most numerous, as targets for UHE proton interactions.

The paper is organized as follows: In Sec. II we discuss the model of the infrared background and its cosmological evolution. In Sec. III we describe the calculation. Section IV gives the results of the calculation, and Sec. V contains the discussion of the results and the conclusions from this research.

II. COSMOLOGICAL EVOLUTION OF THE IR-UV BACKGROUND

It is now well known that galaxies had a brighter past owing to the higher rate of star formation which took place. Strong evolution is supported by many observations relating IR luminosity to the much higher star formation rate at $z \sim 1$ and to the recent determination that most Lyman break galaxies at $z \sim 1$ are also luminous infrared galaxies. In addition to the evolution of galaxy luminosity, some increase in galaxy number density is expected owing to the hierarchical clustering predicted by cold dark matter models. However, luminosity evolution is the dominant effect and it is difficult to separate out a component of density evolution.

*Electronic address: stanev@muon.bartol.udel.edu
†Electronic address: ddm@bartol.udel.edu
‡Electronic address: malkan@astro.ucla.edu
§Electronic address: Floyd.W.Stecker@nasa.gov

In order to calculate intergalactic IR photon fluxes and densities and their evolution over time (or redshift), SMS05 performed an empirically based calculation on the spectral energy distributions of the infrared background radiation by using: (1) the luminosity dependent galaxy spectral energy distributions based on galaxy observations, (2) observationally derived galaxy luminosity distribution functions, and (3) the latest redshift dependent luminosity evolution functions, sometimes referred to as Lilly-Madau plots. The SMS05 calculation was an improved version of the work presented in Refs. [17–19].

The calculation considers two different cosmological evolutions, $\mathcal{E}(z)$ *baseline* and *fast*, of the infrared emission of the type

$$\mathcal{E}(z) = \begin{cases} (1+z)^m: & z < z_{\rm flat} \\ (1+z_{\rm flat})^m: & z_{\rm flat} < z < 6 \\ 0: & z > 6. \end{cases} \quad (1)$$

The *baseline* evolution model is described by $m = 3.1$ and $z_{\rm flat} = 1.3$, while the *fast* evolution model uses $m = 4$ and $z_{\rm flat} = 1$. The infrared emission at $z > z_{\rm flat}$ is constant in both models. Figure 1 shows the number density between photon energy of 3.16×10^{-3} and 1 eV in both models. The *fast* evolution model has higher density in the current cosmological epoch as well at the IRB maximum epoch, which is around $z = 2$. The increase of the total IRB number density increases by a factor of about 4 from $z = 0$ to $z = 2$ and decreases at higher redshifts. One should note, however, that the cosmological evolution of the infrared background density is much slower than that of MBR since the current IRB density is accumulated from the infrared emission of different sources since $z = 6$. Figure 2 shows the energy spectrum of the *fast* infrared background at redshifts from 0 to 5. One can see both the increase of the total photon density as well as the shift of the maximum of the emission to higher energy at higher redshifts. In terms of photoproduction interactions on IRB

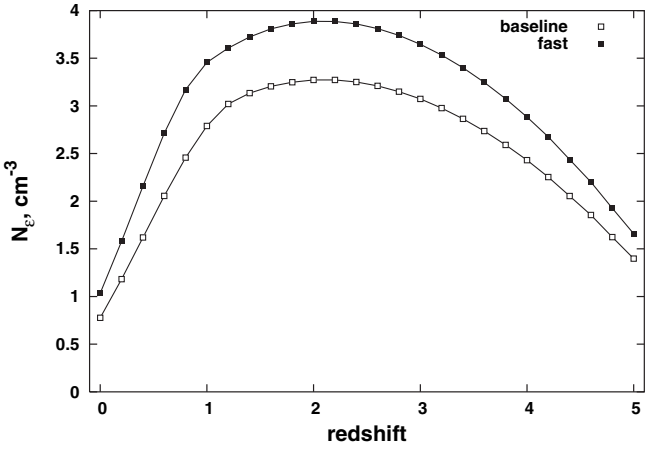

FIG. 1. Number density of the IRB at different redshifts as calculated by SMS05 [16].

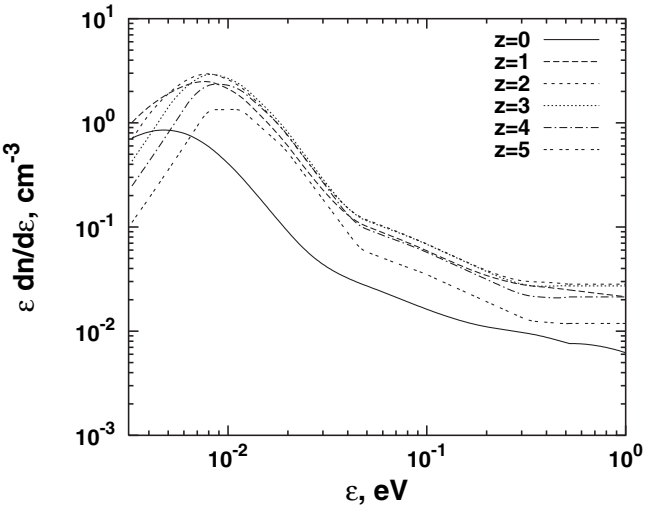

FIG. 2. Number density of the infrared background at different redshifts calculated by SMS05 [16] in the *fast* evolution model.

this means that lower energy cosmic rays will be above the photoproduction threshold at higher redshifts.

Both figures above show the number density of IRB rather than the usual presentation of the energy density. Since we are using the infrared background as a target for cosmic ray interactions this is the relevant quantity.

III. THE CALCULATION

The calculation was performed in two stages: (1) calculation of the neutrino yields from interactions with extragalactic infrared photons and (2) a subsequent integration of the yields to obtain the cosmogenic neutrino flux from such interactions. This approach gives us the flexibility to easily obtain the neutrino flux using different parametrizations of the cosmic ray emissivity, injection spectra, and cosmological evolution of the cosmic ray sources. This approach, however, suffers from the fact that since the yields are calculated only on the IRB, they do not account for the fact that high energy protons interact mainly with the much more numerous MBR photons.

A. Calculation of the neutrino yields

The neutrino yields as a function of the proton energy E_p, neutrino energy E_ν, and the redshift z were calculated using the IRB spectra at different cosmological epochs, i.e., as a function of redshift, that were provided by the authors of Ref. [16]. Each of the yield calculations was performed for proper distances corresponding to $\Delta z = 0.2$ using an $\Omega_M = 0.3$, $\Omega_\Lambda = 0.7$ cosmology as

$$D(z) = \frac{c}{H_0} \int_{z_{\rm min}}^{z_{\rm max}} \frac{1}{1+z} [\Omega_M (1+z)^3 + \Omega_\Lambda]^{-1/2} {\rm d}z. \quad (2)$$

The IRB is considered to be constant during each cosmological epoch of duration $\Delta z = 0.2$.

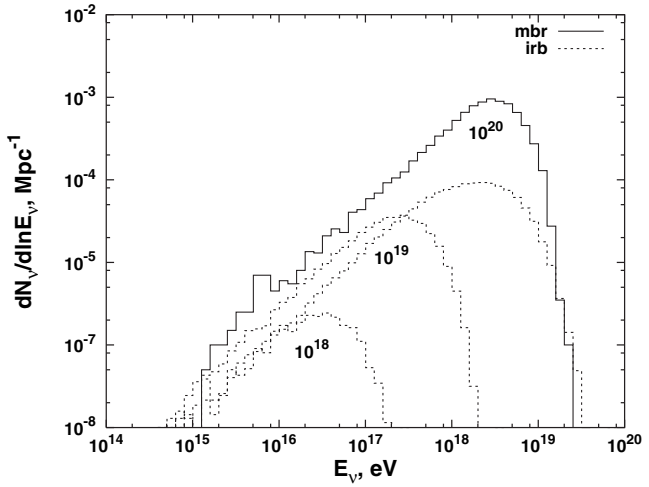

FIG. 3. Neutrino yields for 10^{20} eV protons interacting with both MBR photons and for 10^{18} eV, 10^{19} eV, and 10^{20} eV protons interacting with IRB photons at $z = 0$, given for protons traveling a distance of 1 Mpc.

In this way the matrix element corresponding to $\mathrm{d}t/\mathrm{d}z$ dependence was accounted for in the yields. The yields were calculated with the code used in Ref. [12] and the photoproduction interaction code SOPHIA [20]. All generated neutrinos are redshifted by the code to the end of the Δz epoch. The yields were calculated for redshifts $0 < z < 5$ and for cosmic ray energies above 10^{18} eV in ten logarithmic bins per decade of energy.

Figure 3 compares the ν_μ yields for UHE protons traveling a distance of 1 Mpc and interacting with MBR and IRB photons. The yield for 10^{20} eV protons interacting with IRB photons is about a factor of 10 lower than that for MBR interactions. This difference is much smaller than the ratio of the MBR and IRB total densities, and demonstrates that 10^{20} eV protons interact mainly with photons in the higher frequency Wien tail of the 2.7K MBR spectrum.

Protons of energy 10^{19} eV do not interact at $z = 0$ with MBR photons, but they readily interact and produce neutrinos by interactions with IRB photons, as do protons of energy 10^{18} eV. Even protons of energy 10^{17} eV occasionally interact with IRB photons, but their contribution is very small and is neglected in this calculation. Even for E^{-2} cosmic ray spectra, the smaller 10^{19} and 10^{18} eV yields are multiplied by the much higher flux of cosmic rays with such energies. This is the basis of the significant neutrino (and γ-ray) production from UHECR-IRB interactions.

B. Integration of the yields

The second phase of the calculation requires the parametrization of the redshift evolution of the emissivity of cosmic ray sources and the form of the cosmic ray injection spectrum. We assume a cosmic ray injection spectrum of the power-law form $\mathrm{d}N/\mathrm{d}E_p = AE_p^{-(\gamma+1)} \exp(-E_p/E_{\max})$ with $E_{\max} = 10^{21.5}$ eV.

We consider here two empirically based models for the evolution of UHECR power with redshift, viz., (1) one based on the redshift evolution of the star formation rate that was used in the calculation of the infrared background in SMS05, and (2) the other based on the redshift evolution of flat spectrum radio sources, given as an analytic approximation in Ref. [21]. We use the *fast* evolution model from SMS05 since it is more consistent with the new observations of the Spitzer telescope [22,23].

We normalize the cosmic ray energy flux at $E_p = 10^{19}$ eV to $E_p \mathrm{d}N_p/\mathrm{d}E_p = 2.5 \times 10^{-18}$ cm^{-2} s^{-1} sr^{-1} [24,25]. Since the calculation is extended to energies below 10^{19} eV, the code uses the cosmic ray flux at 10^{19} eV to calculate the injection spectra at lower and higher energy. Therefore, the cosmic ray emissivity above 10^{18} eV depends on the injection spectrum. The injection spectrum itself is used as a free parameter in order to study its influence on the cosmogenic neutrino spectrum.

The integration procedure also has to account for the modification of the cosmic ray spectrum owing to interactions with MBR photons. This was done in two crude, but reasonable, ways. The first one is the introduction of a high energy cutoff of the spectrum as a function of the redshift. The second one, which is used in the results presented below, is to weight the cosmic ray injection spectrum with the interaction length λ_{IRB} on the infrared background radiation. The cosmic rays interacting in the infrared background radiation used in the integration of the yields are $F_{\mathrm{CR}}\lambda_{\mathrm{IRB}}/\lambda_{\mathrm{tot}}$, where λ_{tot} is the interaction length in the total IRB and MBR fields. The fraction of the cosmic ray flux used in the integration procedure is shown in Fig. 4. If one arbitrarily determines the high energy cutoff of the cosmic ray energy spectrum as the energy at which

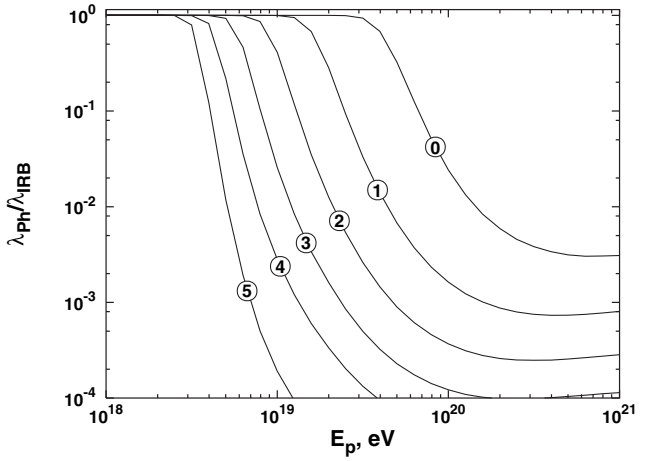

FIG. 4. Fraction of the total cosmic ray flux used in the integration of the neutrino yields from interactions in the IRB. The different lines correspond to fractions at different redshifts as indicated by the numbers in the plot.

only 10% of the cosmic rays interact in the IRB, it would be 7×10^{19} eV at $z = 0$ compared to 2.5×10^{19} and 4×10^{18} eV at $z = 1$ and 5.

Since the yields include the dt/dz factor the integration becomes very simple, viz.:

$$dN_\nu^i/dE_\nu = \int_0^5 dz \times \int^{E_c} \frac{dN_p}{dE_p} \mathcal{E}(z) Y^i[(1+z)E_\nu; E_p, z] dE_p, \quad (3)$$

where the index i indicates the neutrino flavor.

IV. RESULTS

The results of the integration are shown in Fig. 5. The top panel of the figures compares the fluxes of cosmogenic $\nu_\mu + \bar{\nu}_\mu$ neutrinos generated by interactions with MBR photons (filled squares) with those generated by interactions with IRB photons (open squares), assuming a $\gamma = 1$ UHECR injection spectrum with the *fast* evolution of the emissivity of the cosmic ray sources. All panels of Fig. 5 are calculated with the same cosmological evolution. Using the *baseline* evolution model will give neutrino fluxes which are about 25-30% lower.

The peak flux of the IRB-generated neutrinos is not much lower than that of the MBR-generated ones, i.e., 1.7×10^{-17} compared to 2.2×10^{-17} cm^{-2} s^{-1} sr^{-1}. The peak is, however, shifted to lower E_ν by about a factor of 3. The main reason for that shift is the contribution of protons of energy below 3×10^{19} eV to the neutrino production. The IRB-generated neutrino flux is also depleted at energies above 10^{19} eV. This is because protons of energy above 5×10^{19} eV very rarely interact with IRB photons before they lose their energy in MBR interactions. At energies below the peak the IRB-generated neutrino flux is somewhat flatter than the MBR one, although the statistical uncertainty of the calculation does not allow us to make a quantitative statement regarding this.

The middle panel of the figure shows the IRB-generated fluxes of ν_e's and $\bar{\nu}_e$'s assuming an E^{-2} injection spectrum. The electron neutrino flux peaks at the same energy as the muon neutrino one. The $\bar{\nu}_e$ flux, which is due mostly to neutron decay neutrinos, is shifted and widened at its lower energy end. The dip between the ν_e and $\bar{\nu}_e$ peaks is not as deep as it is in the MBR neutrino case. The reason for that is that the ν_e peak is somewhat wider at energies below the peak. The bottom panel of Fig. 5 shows the fluxes of IRB-generated $\nu_\mu + \bar{\nu}_\mu$ assuming a steeper injection spectrum $\gamma = 1.5$ and $m = 3.1$. There are two main differences from the $\gamma = 1$ case. The peak of the IRB-generated neutrino flux is higher by almost a factor of 3 (6.5×10^{-17} in the same units) than for the MBR-generated neutrinos and it is shifted down in energy by a factor of $\sim$3 to $\sim 10^{16.5}$ eV. This is caused by the higher flux of protons of energy below the high energy cutoff. In the case of the MBR-generated neutrinos, the general effect is not as strong but is reversed; the steeper proton spectrum results in a lower flux.

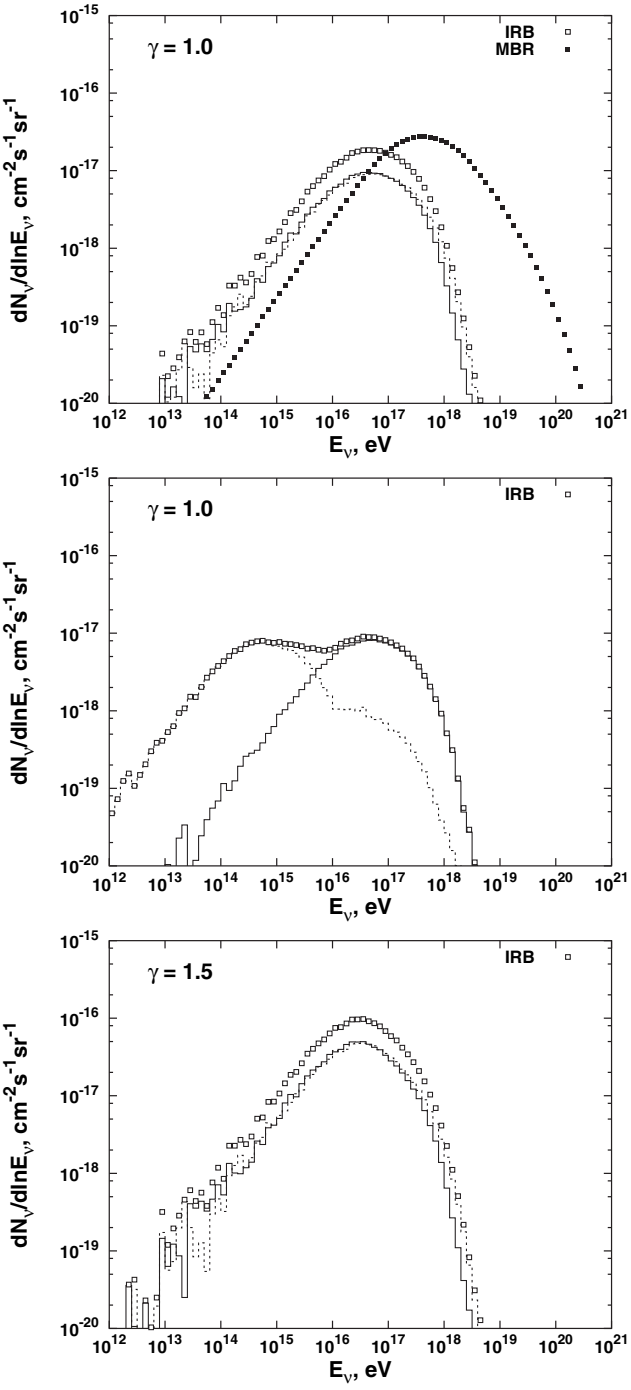

FIG. 5. Top panel: ν_μ (solid) and $\bar{\nu}_\mu$ (dashed) spectra generated by interactions with IRB photons. Their sum (open squares) is compared to those generated by interactions with MBR photons (full squares) for $\gamma = 1$ assuming *fast* evolution of the cosmic ray source emissivity. Middle panel: ν_e (solid) and $\bar{\nu}_e$ (dashed) spectra for injection spectra as in the top panel. Their sum is shown with open squares. Bottom panel: $\nu_\mu + \bar{\nu}_\mu$ spectra for injection spectrum with $\gamma = 1.5$.

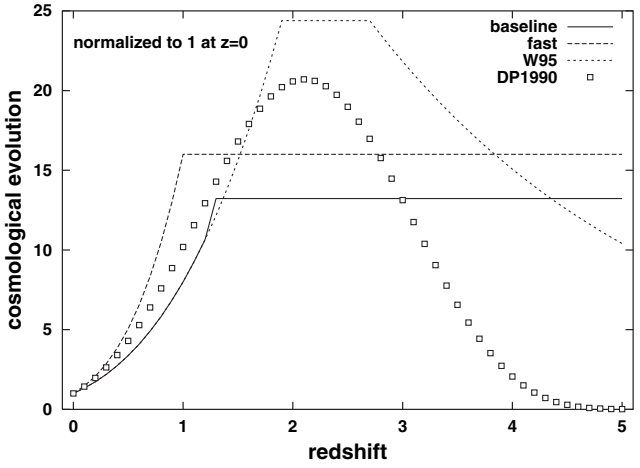

FIG. 6. Four different models for the cosmological evolution of the cosmic ray sources (see text for description and references).

Because of the very strong dependence of the flux of cosmogenic neutrinos on the cosmological evolution of the cosmic ray sources [26], we investigated this dependence further. Figure 6 compares the *baseline* and fast cosmological evolutions of Ref. [16] to those of Refs. [21,24]. All evolution models are normalized to 1 at present, i.e. for $z = 0$.

The evolution taken from Ref. [24], that was used for calculations of the cosmogenic neutrino flux from interactions in the MBR [12], gives a UHECR emissivity which is about 60% higher at redshift of 2 than the average of the models of SMS05. The cosmological evolution of the flat spectrum radio galaxies [21] has an intermediate redshift evolution; it is faster than $m = 3$ and slower than $m = 4$ below $z = 1$ and peaks at about $z = 2$. It is also distinguished by its rapid decrease in emissivity at $z > 3$.

Figure 7 compares the cosmogenic neutrino fluxes of $\nu_\mu + \bar{\nu}_\mu$ generated by the *baseline* and *fast* models of SMS05 with the $m = 3$ model used in Ref. [12] and that of Ref. [21]. The difference in the calculated fluxes is actually quite small, compared to all other uncertainties of the calculation. The *fast* and the *baseline* models bracket from above and from below the fluxes of cosmogenic neutrinos from interactions in the IRB, while the other two models fall between these two. The main reason for the small differences is the dz/dt matrix element that decreases the contribution of higher redshifts, because in the cosmological integration the emissivity is multiplied by the smaller time intervals involved at higher redshifts.

In the case where UHECR luminosity evolution is assumed to be proportional to the redshift distribution of flat spectrum radio galaxies as given in Ref. [21], the neutrino spectra peak at a somewhat higher energy because of the relatively small UHECR emissivity at the higher redshifts.

In Fig. 8 we present the total fluxes of cosmogenic neutrinos from interactions in the MBR and IRB for injection spectra with $\gamma = 1.0$ and 1.5 and for *fast* cosmological evolution of the cosmic ray sources as in Ref. [16].

For a relatively flat ($\gamma = 1$) injection spectrum (empty squares in Fig. 8) interactions with IRB photons generate almost as many cosmogenic neutrinos as interactions on MBR. The peak of the total neutrino energy spectrum from interactions in the MBR and in IRB is shifted to lower energy by a small amount (from 3×10^{17} eV to about 2×10^{17} eV). The distribution extends to lower neutrino energies by more than half a decade.

For steeper spectra ($\gamma = 1.5$) the contribution of IRB-generated neutrinos is more significant and the resulting flux is almost an order of magnitude larger. The magnitude of the flux at the peak of the spectrum is

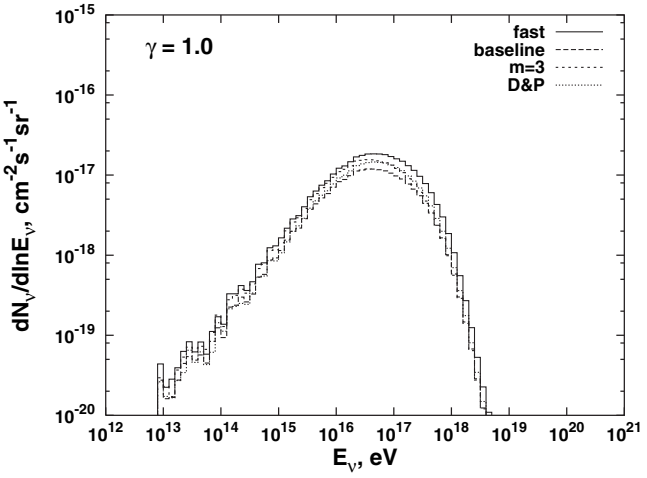

FIG. 7. Cosmogenic neutrino fluxes for four different models of the cosmological evolution of the cosmic ray sources—see text.

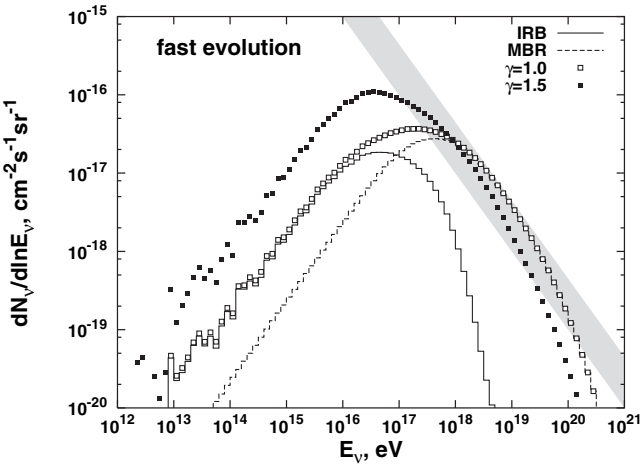

FIG. 8. Total muon $\nu_\mu + \bar{\nu}_\mu$ fluxes for $\gamma = 1.0$ (empty squares) and 1.5 (full squares) calculated with *fast* cosmic ray source evolution. The shaded area represents the W&B [27] upper bound on astrophysical source neutrinos.

$\sim 10^{-16}\,\mathrm{cm}^{-3}\,\mathrm{s}^{-1}\,\mathrm{sr}^{-1}$ and is higher than that of the MBR-generated neutrinos by a factor of ~ 3.

In both cases there is no increase of the neutrino flux at energies exceeding 10^{19} eV. The influence of increased cosmological evolution of the cosmic ray sources is practically the same as in the case of MBR-generated neutrinos alone. In this context, we note that the cosmological evolution of target IR photon density is slower that of the MBR.

For comparison, the shaded area in Fig. 8 shows the upper bound on the astrophysical neutrino spectra given in Ref. [27]. The lower edge is the bound in absence of cosmic ray source cosmological evolution, and the upper edge is for $(1+z)^3$ evolution.

The inclusion of the proton-IRB interactions somewhat reverses the trend of the injection spectrum dependence of the cosmogenic neutrino flux. Without including such interactions, steeper injection spectra lead to smaller cosmogenic neutrino fluxes; with the inclusion of the contribution to the neutrino flux from interactions of IRB photons with relatively lower energy protons, steeper cosmic ray spectra generate higher neutrino fluxes. The reason is that we normalize the cosmic ray injection spectrum at 10^{19} eV, which is now in the middle of the energy range of the interacting cosmic rays. One can see in Fig. 4 the dominance of the interactions in the MBR of cosmic rays of energy above 10^{19} at all redshifts higher than 1. For steeper cosmic ray injection spectra the number of such particles is decreased while that of cosmic rays below 10^{19} eV, that interact in the IRB, is significantly increased.

Because of the lower average energy of the IRB-generated neutrinos, the spectra are shifted and their detectability is lower than that of MBR-generated neutrinos. This is because the neutrino-nucleon cross section rises monotonically with energy. Table I shows the shower rates of ν_e and $\bar{\nu}_e$ CC (charged current) interactions per $\mathrm{km}^3\mathrm{yr}$ of water detector for cosmogenic neutrinos generated by interactions with MBR and IRB photons. These rates are the products of the neutrino cross section times the neutrino flux integrated above E_{sh}. We assume that the total neutrino energy is transferred to the shower initiated by its CC interaction. The calculation of event rates of CC and NC interactions of muon and tau neutrinos are much more difficult and require Monte Carlo models of particular experiments.

TABLE I. Rates per km^3 water per year of showers above different energy generated by different types of neutrino interactions for *fast* cosmological evolution for homogeneously distributed cosmic ray sources (see text).

$\log_{10} E_{\mathrm{sh}}$	$\gamma = 1$		$\gamma = 1.5$	
(GeV) $>$	MBR	IRB	MBR	IRB
6	0.092	0.021	0.078	0.085
7	0.088	0.019	0.072	0.072
8	0.079	0.010	0.063	0.030
9	0.044	0.001	0.027	0.001
10	0.008	0.000	0.003	0.000

The second column of Table I corresponds to the numbers given in a similar table in Ref. [12]. The numbers cannot be directly compared because of the different cosmologies ($\Omega_M = 1$ in Ref. [12] and $\Omega_M = 0.3$ here) and cosmological evolutions of the cosmic ray sources used. The $\Omega_M = 0.3$ cosmology increases the neutrino rates by about 70%.

In the $\gamma = 1.0$ injection case the rates from MBR neutrinos are higher by factors above 4 at all shower thresholds, while in the $\gamma = 1.5$ case the IRB rates are higher or similar for shower thresholds below 10^8 GeV. Above that energy MBR neutrinos generate higher rate. Note that IRB neutrinos do not contribute at all to the shower rates above 10^9 GeV.

The total shower rate for $E_{\mathrm{sh}} > 10^6$ GeV is higher than the MBR only rate by about 20% in the $\gamma = 1.0$ case, while in the $\gamma = 1.5$ case it more than doubles the detection rate.

Most of the contemporary fits of the injection spectrum of the highest energy cosmic rays confirm the conclusion of Ref. [28] that it is steeper than E^{-2}. The spectrum derived by these authors is $E^{-2.7}$ with a significant flattening at about 10^{18} eV, which could be explained with different effects, see e.g. Ref. [29]. The shape of the spectrum may be accounted for in this model as a result of the $p\gamma \rightarrow e^+e^-$ process [30] as discussed in Ref. [31]. This pair production process creates a dip at about 10^{19} eV and a slight excess at the transition from pair production to purely adiabatic proton energy loss at about 10^{18} eV. This fit does not require a strong cosmological evolution of the cosmic ray sources but can accommodate a mild one $\propto (1+z)^m$ with $m \leq 3$ [32]. In the case of a flatter injection spectrum the pair production dip is well fit also by $m = 4$.

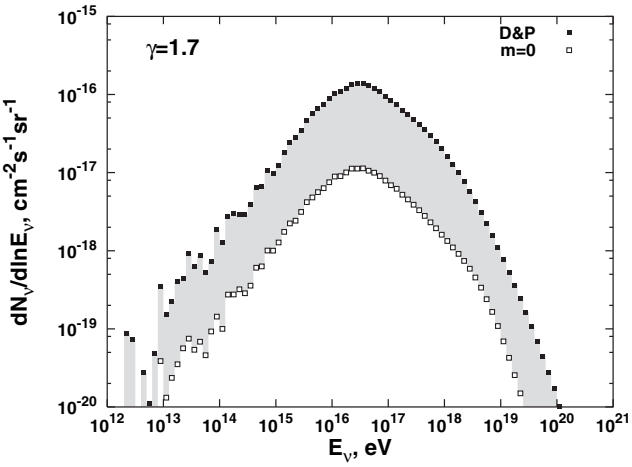

FIG. 9. Total muon $\nu_\mu + \bar{\nu}_\mu$ fluxes for $\gamma = 1.7$ and evolution from Ref. [21] source evolution (full squares) and no evolution (empty squares).

Figure 9 shows the spectra of the cosmogenic neutrinos from interactions with MBR and IRB photons assuming a steep injection spectrum with $\gamma = 1.7$ and (1) no evolution with ($m = 0$) and (2) evolution according to Ref. [21]. The difference between the two neutrino spectra is significant; the peak values are 10^{-17} and 1.5×10^{-16} cm^{-2} s^{-1} sr^{-1} for without and with evolution. The addition of the IRB component brings these spectra into the range of detectability, especially in the case of mild cosmological evolution.

V. DISCUSSION AND CONCLUSIONS

The evolution models of SMS05 do not give the highest IRB-generated neutrino flux. We compared the IRB photon density in this model with the models of Refs. [33,34]. Both of these models have higher IRB density in the relevant energy range between 3×10^{-3} and 1 eV. The total IRB densities in this range are 1.27 [33] and 1.12 [34] compared with the density of 1.03 used here. In addition, Ref. [34] shows somewhat faster cosmological evolution. The use of any of these models would have increased somewhat the calculated flux of cosmogenic neutrinos. The uncertainty in the IRB flux is of the order of 30% [16], while the biggest uncertainty in this calculation is in the UHECR flux and its cosmological evolution.

The IRB contribution to the total cosmogenic neutrinos flux can be increased slightly as protons of energy below 10^{18} eV can interact with IRB photons and generate lower energy neutrinos. If such interactions were included the IRB spectrum would be wider than the MBR one, especially at energies below 10^{16} eV.

It is difficult to compare our results with those of Refs. [14,15] because of the different astrophysical input in these calculations. Qualitatively the results of these calculations are similar to ours and certainly agree within a factor of 2.

In conclusion, we calculated the flux of cosmogenic neutrinos from interactions of UHECR protons with IRB photons using the recent calculations of IR photon spectra densities as a function of redshift by SMS05. Our calculations show that UHECR interactions with IRB photons produce a significant flux of cosmogenic neutrinos, one which is comparable to interactions with MBR photons. This is especially true in the case of assumed steep injection spectra of the ultrahigh energy cosmic rays. The total neutrino event rates at energies above 1 PeV increase by more than a factor of 2 in the case of injection spectra with $\gamma = 1.5$. Because of the much lower mean free path of protons above 10^{20} eV in the MBR interactions with IRB photons do not increase the higher energy end of the cosmogenic neutrino spectrum. The total cosmogenic fluxes, however, are still not detectable with conventional neutrino telescopes such as IceCube [35] or the European km^3 telescope [36]. A reliable detection is only expected from radio [37] and acoustic neutrino detectors.

ACKNOWLEDGMENTS

We thank Tanja Kneiske for sharing with us the tables of cosmological evolution of the IR background from Ref. [34]. This work was supported in part by NASA Grants No. ATP03-0000-0057 and No. ATP03-0000-0080.

Note added in proof.—After completion of this paper, SMS05 was revised using a slightly revised evolution function and 60μ infrared galaxy luminosity function. Had we used these new revisions, they would have changed our results only slightly and by amounts which are much smaller than the uncertainty in the cosmological evolution of the ultrahigh energy cosmic ray sources.

[1] V. S. Berezinsky and G. T. Zatsepin, Phys. Lett. **28B**, 423 (1969); Sov. J. Nucl. Phys. **11**, 111 (1970).
[2] K. Greisen, Phys. Rev. Lett. **16**, 748 (1966); G. T. Zatsepin and V. A. Kuzmin, JETP Lett. **4**, 78 (1966).
[3] F. W. Stecker, Astrophys. Space Sci. **20**, 47 (1973).
[4] F. W. Stecker, Astrophys. J. **228**, 919 (1979).
[5] J. Wdowczyk, W. Tkaczyk, and A. W. Wolfendale, J. Phys. A: Gen. Phys. **5**, 1419 (1972).
[6] V. S. Berezinsky and A. Yu. Smirnov, Astrophys. Space Sci. **32**, 461 (1975).
[7] V. S. Berezinsky and G. T. Zatsepin, Sov. J. Uspekhi **20**, 361 (1977).
[8] C. T. Hill and D. N. Schramm, Phys. Rev. D **31**, 564 (1985).
[9] C. T. Hill, D. N. Schramm, and T. P. Walker, Phys. Rev. D **34**, 1622 (1986).
[10] S. Yoshida and M. Teshima, Prog. Theor. Phys. **89**, 833 (1993).
[11] R. J. Protheroe and P. A. Johnson, Astropart. Phys. **4**, 253 (1996).
[12] R. Engel, D. Seckel, and T. Stanev, Phys. Rev. D **64**, 093010 (2001).
[13] T. Stanev, Phys. Lett. B **595**, 50 (2004).
[14] E. V. Bugaev, A. Misaki, and K. Mitsui, Astropart. Phys. **24**, 345 (2005).
[15] E. V. Bugaev and P. A. Klimai, astro-ph/0509395.
[16] F. W. Stecker, M. A. Malkan, and S. T. Scully, astro-ph/0510449v2.
[17] M. A. Malkan and F. W. Stecker, Astrophys. J. **496**, 13 (1998).
[18] M. H. Salamon and F. W. Stecker, Astrophys. J. **493**, 547 (1998).

[19] M. A. Malkan and F. W. Stecker, Astrophys. J. **555**, 641 (2001).
[20] A. Mucke, R. Engel, J. P. Rachen, R. J. Protheroe, and T. Stanev, Comput. Phys. Commun. **124**, 290 (2000).
[21] J. S. Dunlop and J. A. Peacock, Mon. Not. R. Astron. Soc. **247**, 19 (1990).
[22] P. G. Pérez-Gonzalez *et al.*, Astrophys. J., **630**, 82 (2005).
[23] E. Le Floc'h *et al.*, Astrophys. J. **632**, 169L (2005).
[24] E. Waxman, Astrophys. J. **452**, L1 (1995).
[25] F. W. Stecker and S. T. Scully, Astropart. Phys. **23**, 203 (2005).
[26] D. Seckel and T. Stanev, Phys. Rev. Lett.,**95**, 141 101 (2005).
[27] E. Waxman and J. N. Bahcall, Phys. Rev. D **59**, 023002 (1999).
[28] V. S. Berezinsky, A. Z. Gazizov, and S. I. Grigorieva, Phys. Lett. B **612**, 147 (2005); see also hep-ph/0204357 and astro-ph/0210095.
[29] R. Aloisio and V. S. Berezinsky, Astrophys. J. **625**, 249 (2005).
[30] G. R. Blumenthal, Phys. Rev. D **1**, 1596 (1970).
[31] V. S. Berezinsky and S. I. Grigorieva, Astron. Astrophys. **199**, 1 (1988).
[32] D. De Marco and T. Stanev, Phys. Rev. D **72**, 081301 (2005).
[33] A. Franceschini *et al.*, Astron. Astrophys. **378**, 1 (2001).
[34] T. M. Kneiske, K. Mannheim, and D. H. Hartman, Astron. Astrophys. **386**, 1 (2002).
[35] ICECUBE project: http://icecube.wisc.edu.
[36] KM3NeT consortium: http://www.km3net.org.
[37] H. Falke, P. Gorham, and R. J. Protheroe, New Astron. Rev. **48**, 1487 (2004).